Supporting Information for

Layer-structured $BaTiO_3$/P(VDF-HFP) composites with concurrently improved dielectric permittivity and breakdown strength toward capacitive energy-storage applications

Liang Sun[a], Zhicheng Shi[a,*], Liang Liang[a], Shuang Wei[a], Huanlei Wang[a], Davoud Dastan[c,*], Kai Sun[b], Runhua Fan[b].

[a]School of Materials Science and Engineering, Ocean University of China, Qingdao 266100, P. R. China

[b]Institute of Marine Materials Science and Engineering, Shanghai Maritime University, Shanghai 201306, P. R. China

[c]School of Materials Science and Engineering, Georgia Institute of Technology, Atlanta, Georgia-30332, USA

[*]Corresponding author: Zhicheng Shi; Davoud Dastan

[*]E-mail: zcshi@ouc.edu.cn; davoud.dastan@mse.gatech.edu

Key words: Polymer composites; Dielectric property; Multilayer structure; Film capacitor; Interfacial polarization.

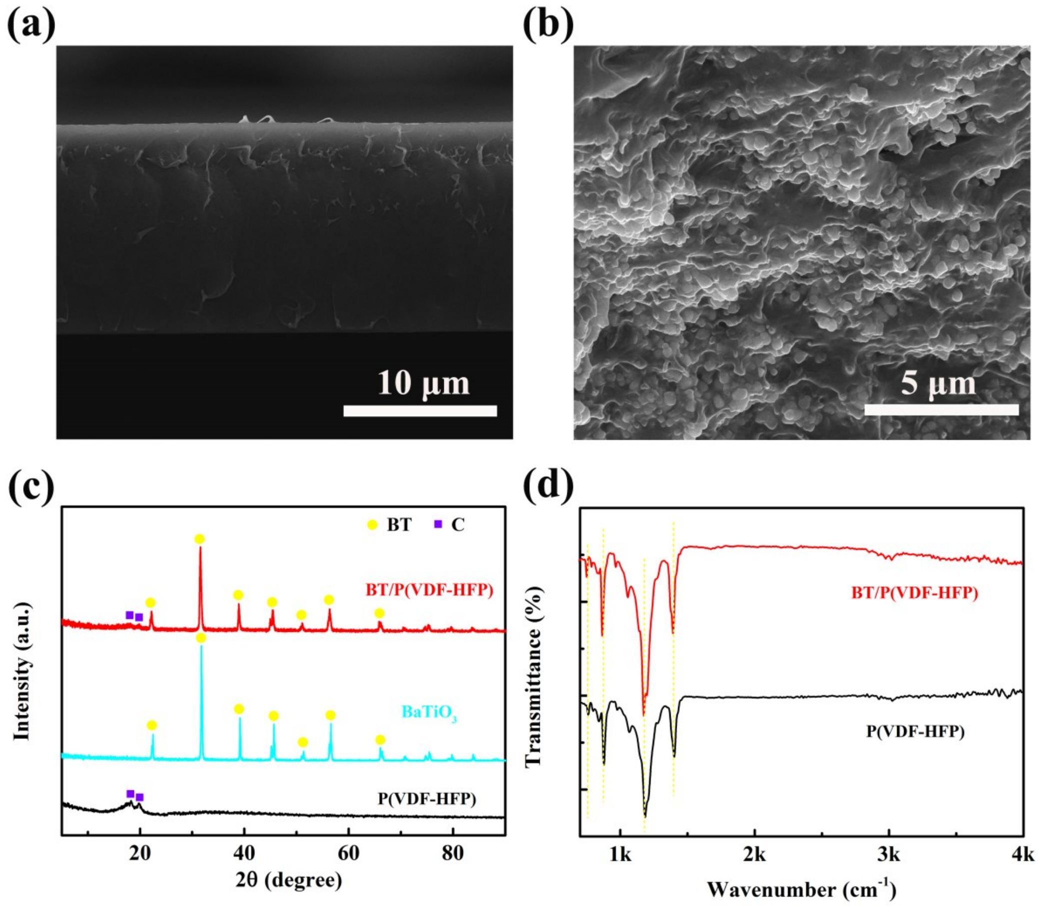

Fig. S1 Cross-sectional SEM morphologies of (a) pure P(VDF-HFP) and (b) single-layer BT/P(VDF-HFP) composite with 15 vol% BT; (c) XRD of pure P(VDF-HFP), single-layer BT/P(VDF-HFP) composite with 15 vol% BT and $BaTiO_3$ nanoparticals;(d) FT-IR of pure P(VDF-HFP) and single-layer BT/P(VDF-HFP) composite with 15 vol% BT.

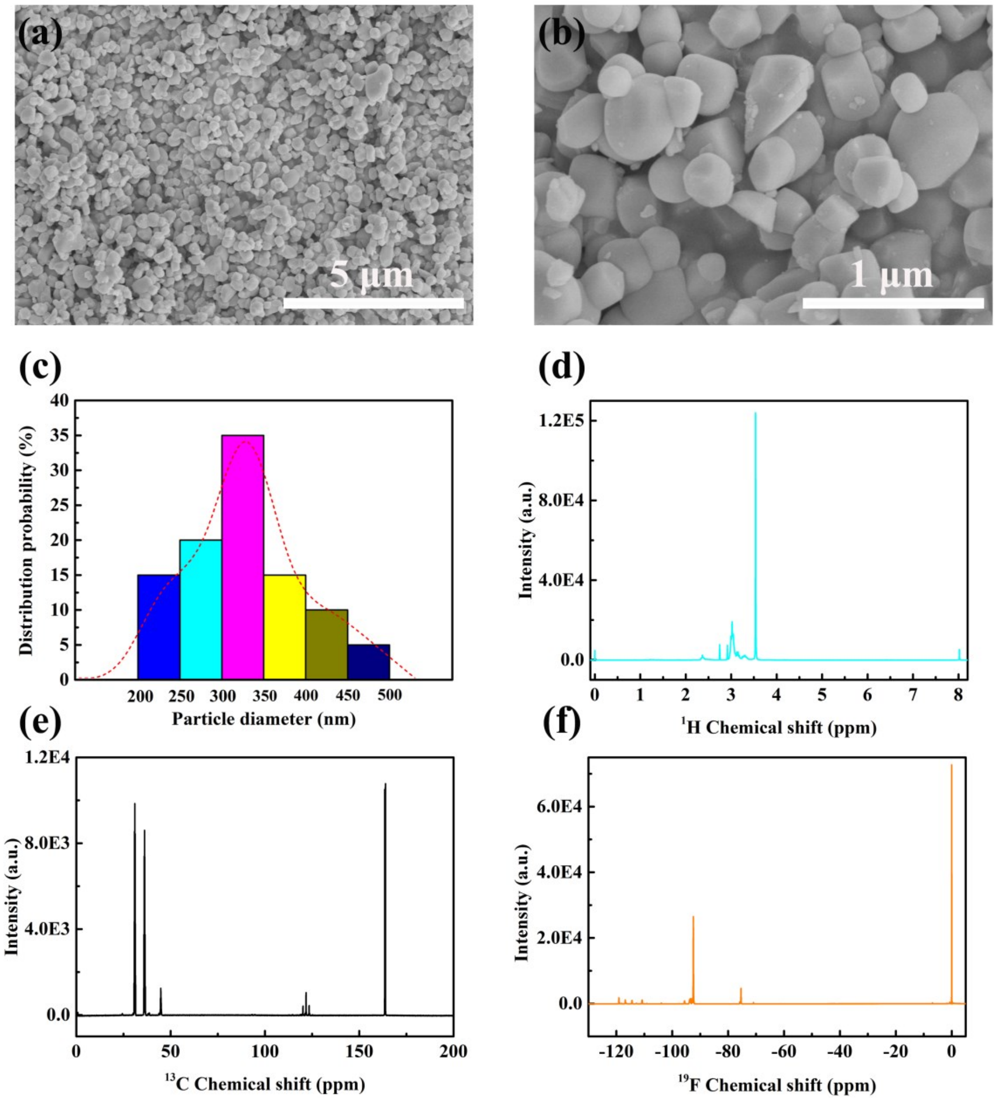

Fig. S2 (a.b) SEM and (c) size distribution of $BaTiO_3$ nanoparticles; (d)^{1}H spectrum, (e)^{13}C spectrum and (f)^{19}F spectrum of pure P(VDF-HFP).

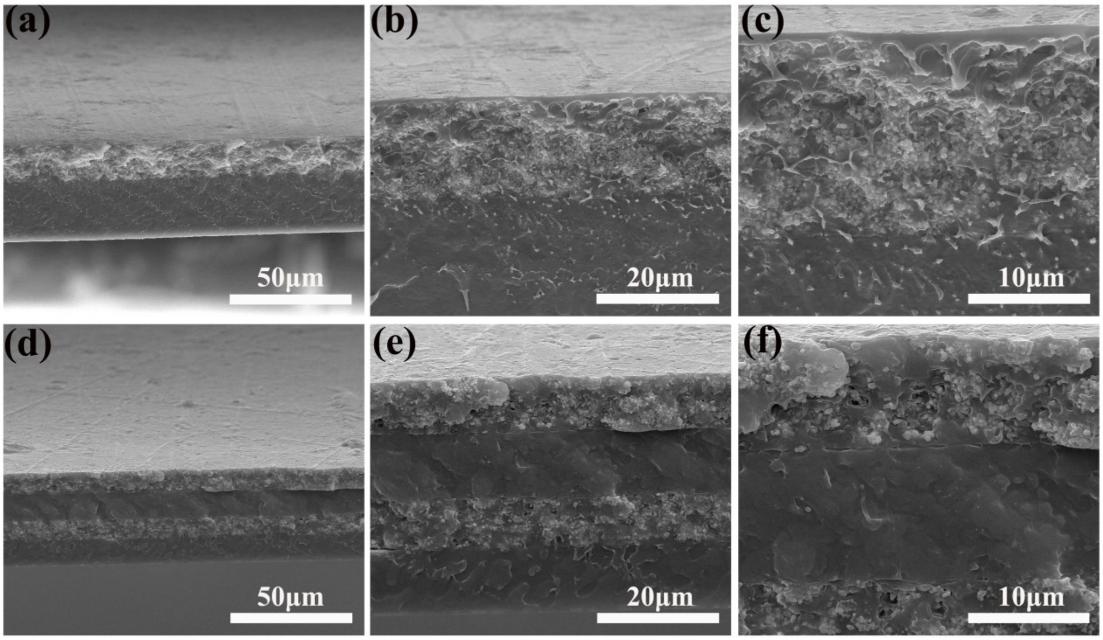

Fig. S3 Cross-sectional SEM morphologies of (a-c) 2-layer and (d-f) 4-layer BT/P(VDF-HFP) composites with 15 vol% $BaTiO_3$.

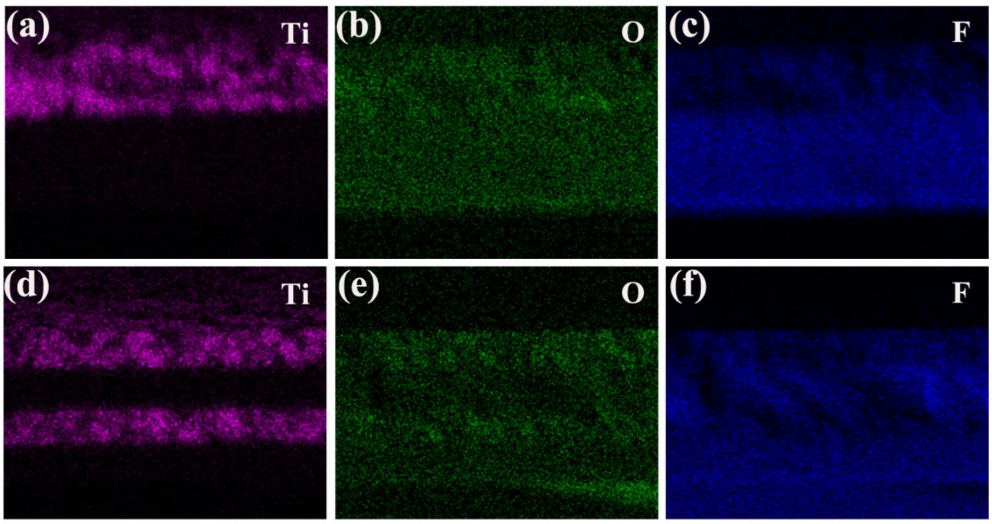

Fig. S4 (a-c) EDX mapping of 2-layer and (d-f) 4-layer composites with 15 vol% BT.

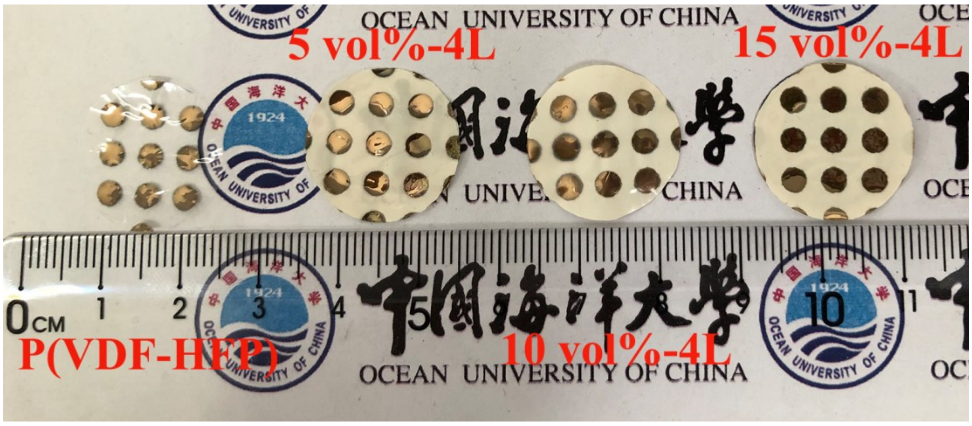

Fig. S5 Optical photograph of P(VDF-HFP) and 4-layer BT/P(VDF-HFP) with 5 vol%, 10 vol% and 15 vol% BT.

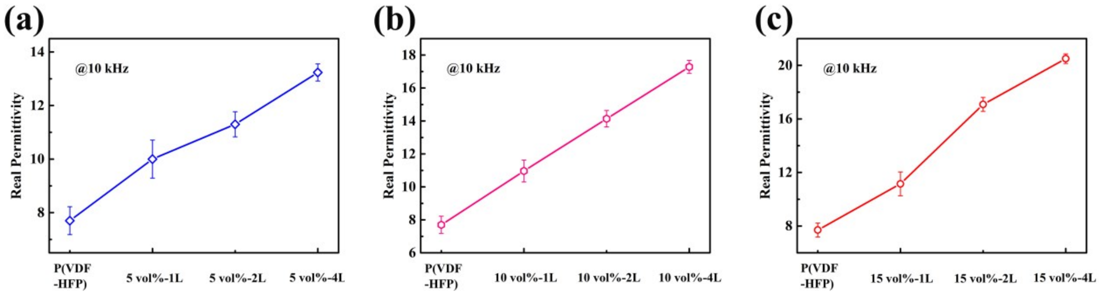

Fig. S6 The dielectric permittivity standard deviations of (a) 5 vol% BT/P(VDF-HFP), (b) 10 vol% BT/P(VDF-HFP) and (c) 15 vol% BT/P(VDF-HFP) composites with different number of layers.

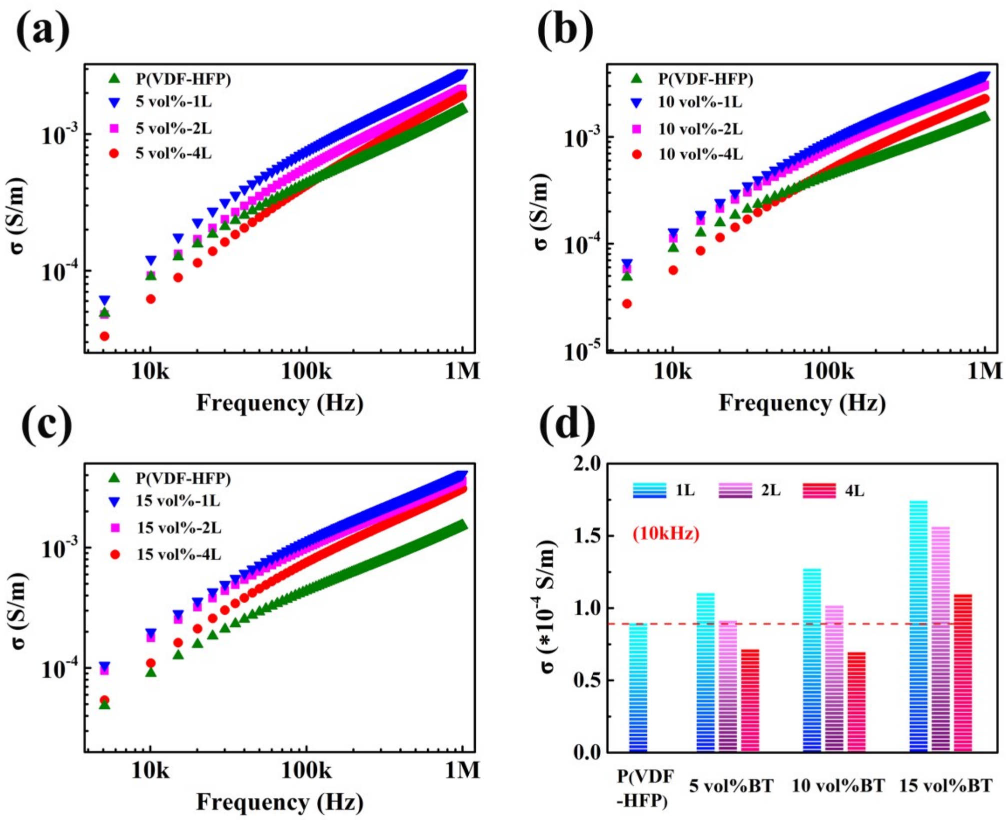

Fig. S7 (a-c) Frequency dependences of the electrical conductivity for for 5 vol% BT/P(VDF-HFP), 10 vol% BT/P(VDF-HFP) and 15 vol% BT/P(VDF-HFP) composites with different number of layers. (d) Electrical conductivity of the 1-layer，2-layer and 4-layer composites with different BT loadings at 10 kHz.

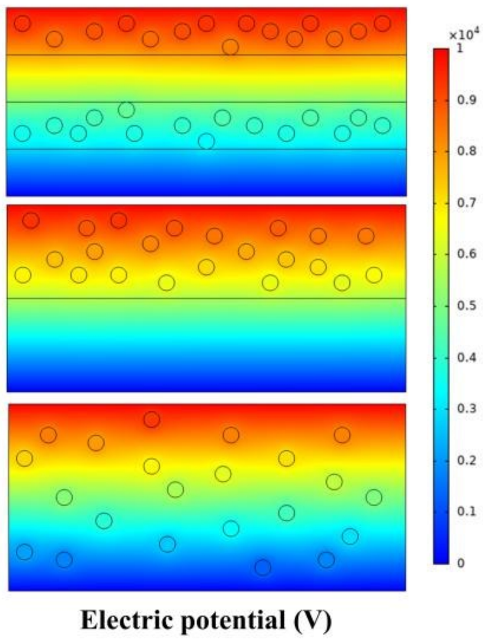

Fig. S8 The distribution of electric potential in 1-layer, 2-layer and 4-layer composites by finite element simulation.

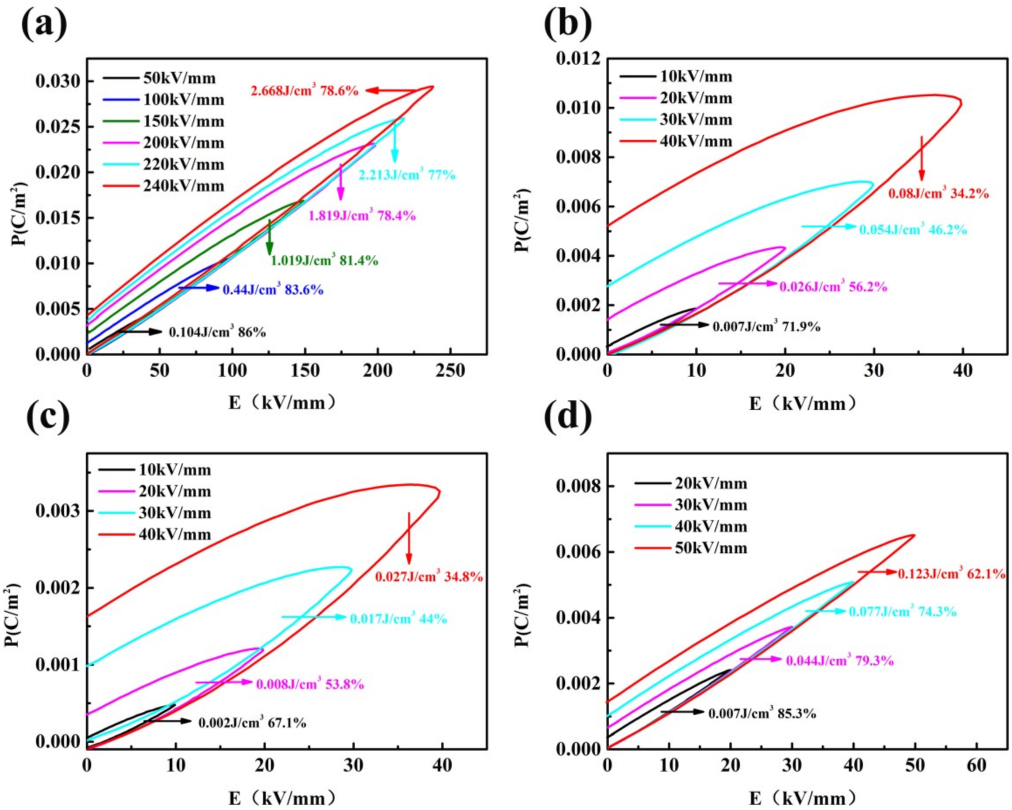

Fig. S9 *P*-*E* loops of pure P(VDF-HFP) and 1-layer composites with different loading fractions of BT under varied electric fields.

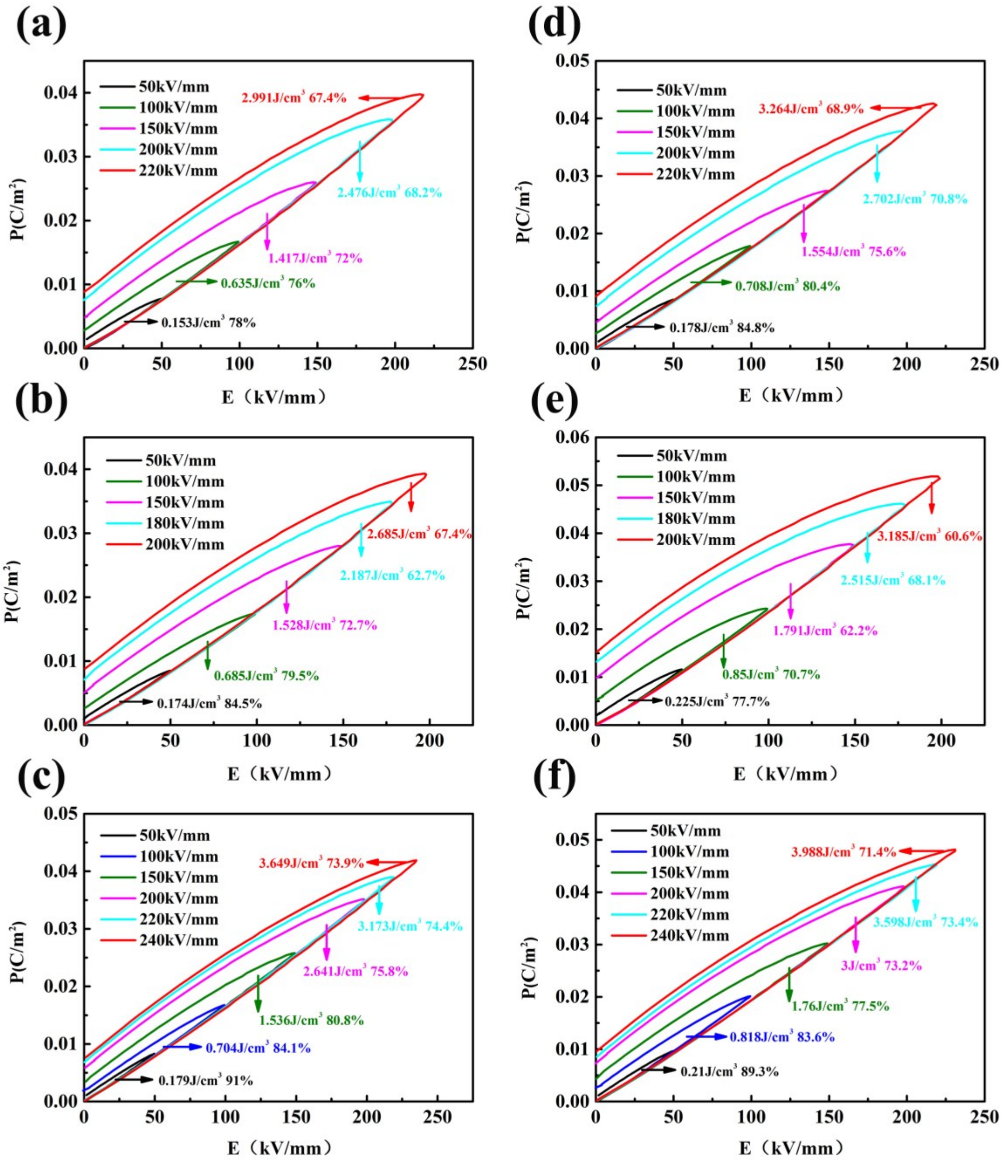

Fig. S10 (a-c) *P*-*E* loops of 2-layer and (d-f) 4-layer composites with different loading fractions of BT under varied electric fields.

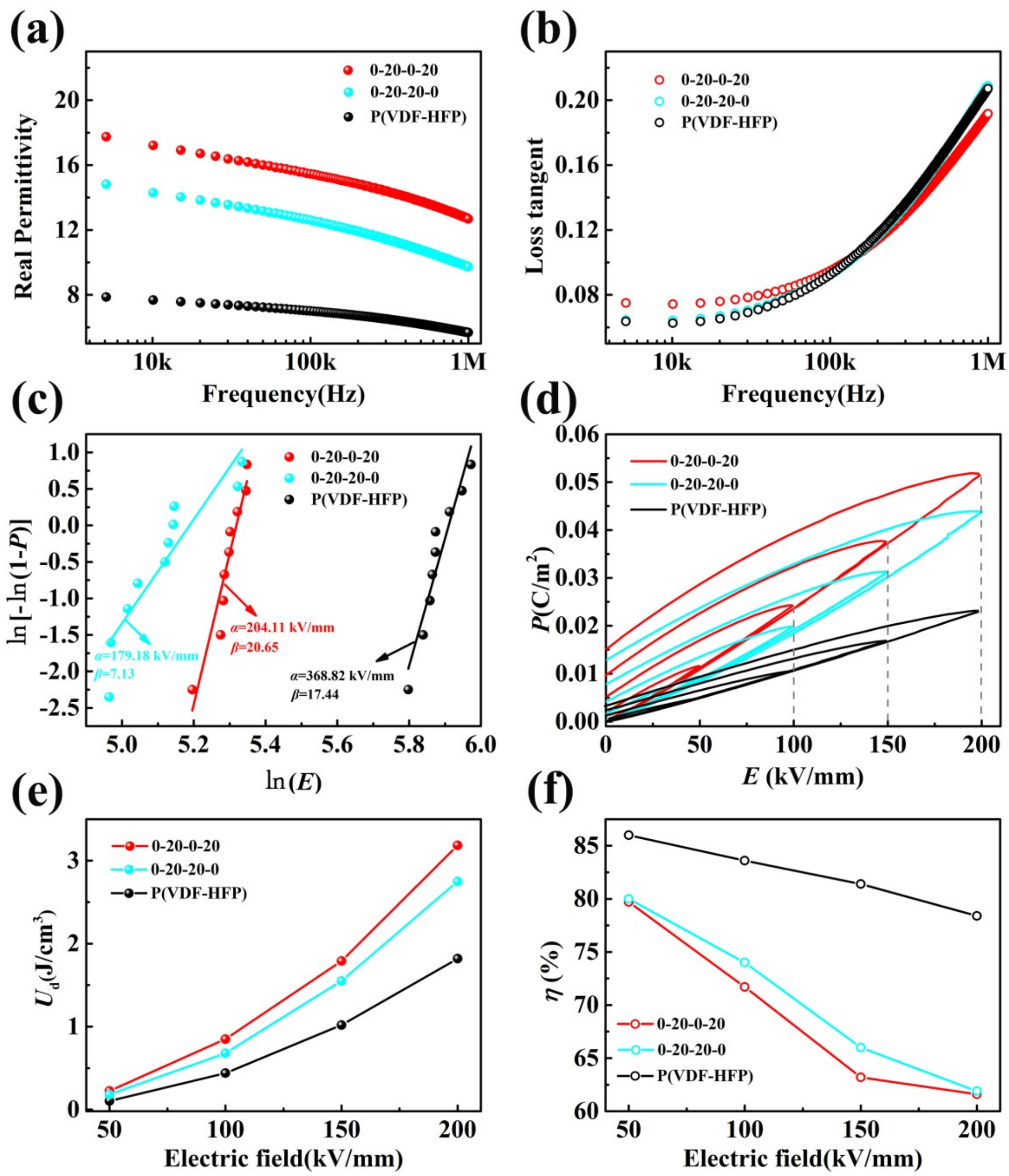

Fig. S11 Frequency dependences of (a) dielectric permittivity and (b) loss tangent for 4-layer composites with different stacking order; (c) Weibull distribution plots of 4-layer composites;(d) *P*-*E* loops of 4-layer composites under varied electric fields; (e)The discharged energy densities and (f) discharged efficiencies of 4-layer composites under varied external electric fields.

As shown in Figure S11, the 0-20-0-20 composite exhibits better comprehensive dielectric energy storage performances than the 0-20-20-0 composite.